



## Investigation of Circular Dichroism in Asymmetric Metamaterial

Priyanka Das<sup>(1)</sup> and Gaurav Varshney<sup>(2)</sup>

(1) EEE Department, Indian Institute of Technology Guwahati

(2) ECE Department, National Institute of Technology Patna

### Abstract

This article demonstrates asymmetric transmission in a chiral metamaterial across 7-11 GHz. When right-handed circularly polarized (RCP) and left-handed circularly polarized (LCP) waves impinge on this chiral metasurface, they exhibit different transmission characteristics. Non-reciprocity is observed when the RCP and LCP waves are incidents on the back side of the proposed metamaterial. Maximum circular dichroism is observed at 8.8 GHz for incident CP waves on the front side of the metamaterial. For waves impinging on the back side of the metamaterial, maximum circular dichroism is observed at 7.86 GHz and 10.06 GHz with the polarization plane rotated by  $27.3^\circ$  in the clockwise direction and  $59^\circ$  in the anticlockwise direction, respectively. Numerical simulations based on finite integration technique have been used to demonstrate circular dichroism. The proposed chiral metamaterial is a potential candidate for bio-sensing applications.

### 1. Introduction

Chirality is exhibited by metamaterials which do not possess two-fold rotational symmetry [1]. The mirror symmetry plane is absent in chiral metamaterials as a result of which the polarization plane of incident electromagnetic waves is rotated [2,3]. Circular dichroism has been obtained by using Y-shaped [4], twisted semicircular shaped [5] and twisted Z shaped [6] structures. Chirality generates negative refractive index for circularly polarized waves [7] which makes them suitable for optical applications.

In this paper, circular dichroism is demonstrated in the frequency band 7-11 GHz, using bi-layered twisted S-shaped structures. A planar metamaterial with intrinsic chirality is proposed. Linearly polarized (LP) waves are converted into elliptically polarized waves by the proposed metamaterial while circularly polarized (CP) waves exhibit transmission asymmetry while propagating through it.

### 2. Design and analysis of chiral metamaterial

A planar chiral metamaterial with non-superimposable mirror images is proposed. The structure of metamaterial

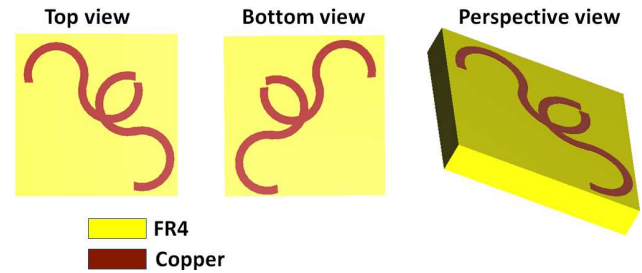


Fig. 1 Structure of the unit cell

unit cell having lateral dimensions  $10 \text{ mm} \times 10 \text{ mm}$  is depicted in Fig. 1. The top copper pattern comprises twisted S-shaped structures of thickness 0.5 mm which are inclined at an angle of  $45^\circ$  with the vertical. The outer and inner radii of curvature of the semicircular metallic portions are 2 mm and 1.5 mm respectively. In the top layer, the copper pattern is constructed by combining an inclined S shaped structure with its non-superimposable mirror image along the diagonal. The copper pattern in the bottom layer is formed by rotating the copper pattern in the top layer by  $90^\circ$ . The dielectric substrate used is FR4 having a thickness of 1.6 mm and relative permittivity of 4.4. Circular dichroism is measured by the difference in transmission coefficient of right hand circularly polarized (RCP) and left hand circularly polarized (LCP) waves. A maximum value of circular dichroism is obtained at 8.8 GHz, as shown in Fig. 2. The transmission coefficient of RCP waves is higher than LCP waves in the frequency range 7.7-10.1 GHz while it is lower than LCP waves in the frequency range 7-7.6 and 10.2-10.8 GHz.

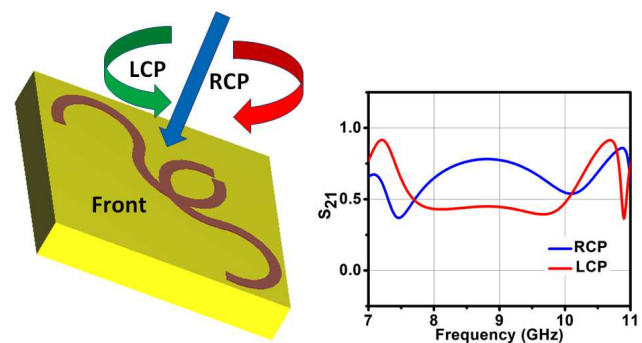


Fig. 2 Transmission characteristics for EM waves incident on the front surface.

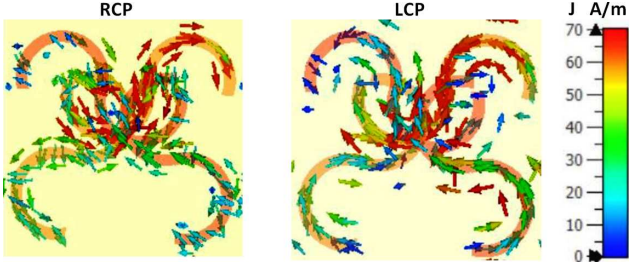


Fig. 3 Current distribution at 8.8 GHz for incident CP waves on the front side.

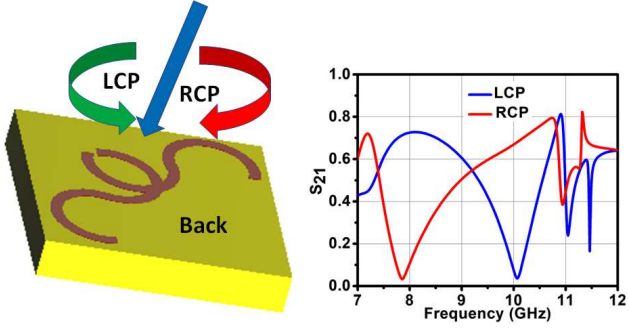


Fig. 4 Transmission characteristics for EM waves incident on the back surface.

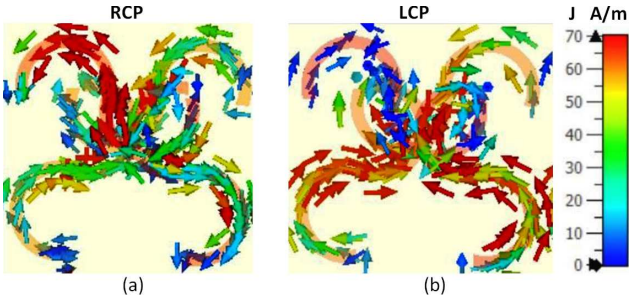


Fig. 5 Current distribution (a) at 7.86 GHz for incident RCP waves on the back side. (b) at 10.06 GHz for incident LCP waves on the back side.

The incident electric field of RCP and LCP waves on the front surface creates a magnetic dipole by forming oppositely directed currents in the top and bottom layer as shown in Fig. 3. Non-reciprocity is observed due to asymmetry in the proposed metamaterial. CP waves incident on the back of the structure exhibit transmission characteristics which are different from the waves incident on the top layer. Maximum circular dichroism is obtained at 7.86 GHz and 10.06 GHz as shown in Fig. 4. Incident RCP and LCP waves excite antisymmetric resonance modes at 7.86 GHz and 10.06 GHz respectively, thereby forming oppositely directed currents, as evident from Fig. 5. The degree of circular dichroism varies with change in the incidence angle for both forward and backward propagating EM waves in the operating frequency range 7-11 GHz as demonstrated in Fig. 6 and Fig. 7 respectively. With increase in incidence angle, circular dichroism is enhanced with minimum value at  $0^\circ$  and maximum value at  $60^\circ$ .

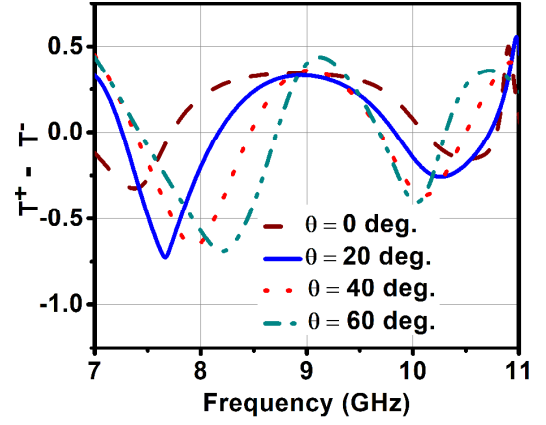


Fig. 6 Angular stability in circular dichroism for incident waves on the front surface.

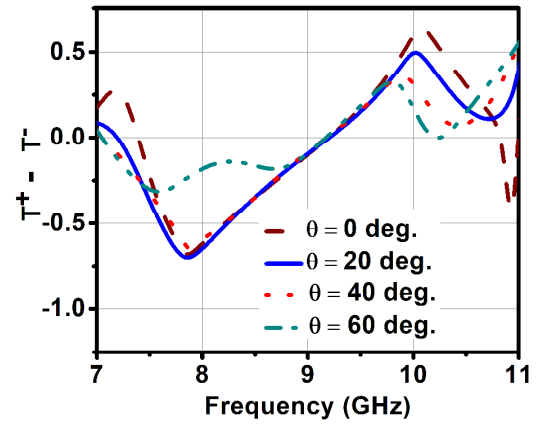


Fig. 7 Angular stability in circular dichroism for incident waves on the back surface.

The polarization rotation angle ( $\theta$ ) for CP waves is given by (1).

$$\theta = \frac{\text{phase}(T^+) - \text{phase}(T^-)}{2} \quad (1)$$

where  $T^+$  is the transmission coefficient for RCP waves and  $T^-$  is the transmission coefficient for LCP waves. Polarization rotation angle ( $\theta$ ) is  $25^\circ$  at 7.6 GHz for CP waves incident on the front surface as shown in Fig. 8. Polarization rotation in the anticlockwise direction is obtained below 9 GHz. Maximum value of  $\theta$  at 10 GHz is  $18.5^\circ$  in the clockwise direction. For CP waves incident on the back surface of the proposed metamaterial,  $\theta$  is in the clockwise direction from 7.5-9.8 GHz as shown in Fig. 9. At 9.8 GHz,  $\theta$  acquires a maximum value of  $90^\circ$  in the anticlockwise direction.

The ellipticity angle ( $\phi$ ) is given by (2).

$$\phi = \tan^{-1} \left( \frac{|T^+| - |T^-|}{|T^+| + |T^-|} \right) \quad (2)$$

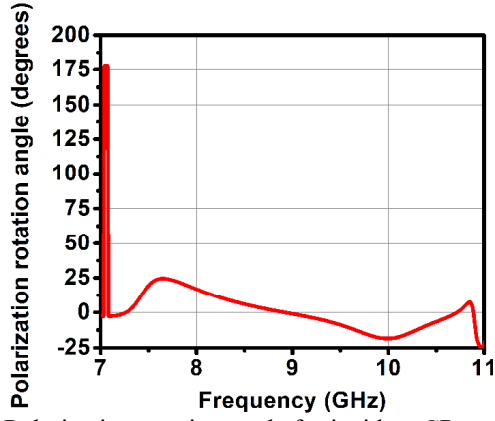


Fig. 8 Polarization rotation angle for incident CP waves on the front surface.

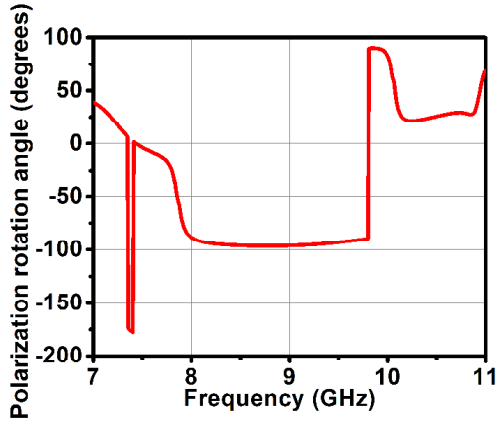


Fig. 9 Polarization rotation angle for incident CP waves on the back surface.

At 7.4 GHz,  $\varphi = -18^\circ$  and at 9.3 GHz,  $\varphi = 15^\circ$ . Ellipticity angle is negative from 7-7.7 GHz and positive above 7.7 GHz till 10 GHz for CP waves incident on the metasurface front side. This is shown in Fig. 10. For CP incidence on the back side of the metamaterial,  $\varphi$  is negative from 7.4-9.2 GHz and positive in the frequency range 9.2-10.8 GHz as shown in Fig. 11. At 10.1 GHz,  $\varphi$  acquires a maximum value of  $41^\circ$ . At 7.86 GHz,  $\varphi$  acquires a minimum value of  $-42.4^\circ$ .

The proposed metamaterial behaves differently for TE and TM polarized waves incident on the front surface. As evident from Fig. 12, transmission of TE incident (y-polarized) waves is maximum at 7.5 GHz and minimum at 9.85 GHz. Transmission of TM incident (x-polarized) waves is maximum at 9.8 GHz and minimum at 7.6 GHz.

$$T^\pm = \frac{T_{yy} \mp iT_{xy}}{\sqrt{2}} \quad (3)$$

where  $T_{yy}$  is the transmission coefficient of y-polarized incident EM waves and  $T_{xy}$  is the transmission coefficient of x-polarized EM waves for y-polarized incident waves. At 7.6 GHz and 9.8 GHz, linearly polarized waves are converted into left-handed and right-handed elliptically polarized waves. A phase difference of  $90^\circ$  and  $-270^\circ$  exists between TE (y-polarized) and TM (x-polarized) waves at 7.6 GHz and 9.8 GHz respectively, as evident from Fig. 13.

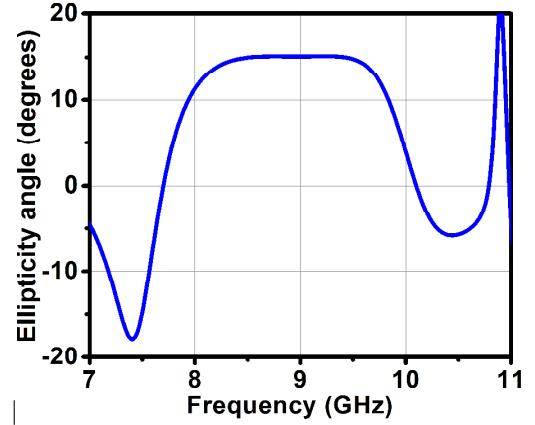


Fig. 10 Ellipticity angle for incident CP waves on the front surface.

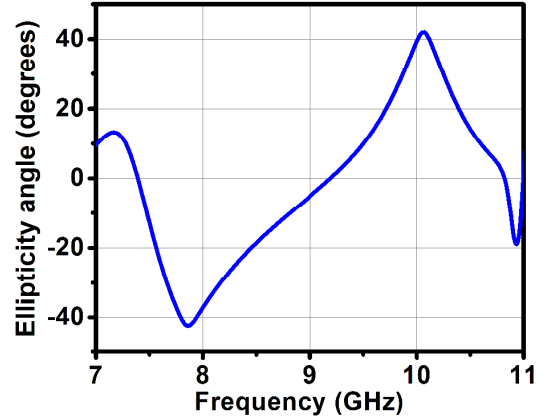


Fig. 11 Ellipticity angle for incident CP waves on the back surface.

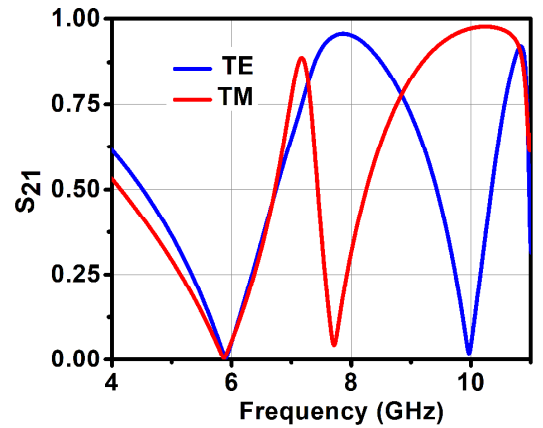


Fig. 12 Frequency response of linearly polarized waves.

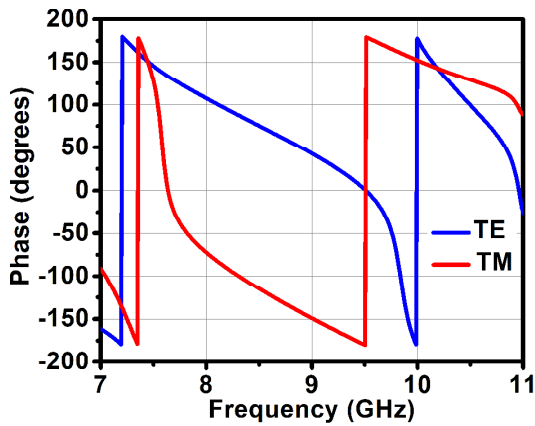


Fig. 13 Phase response of linearly polarized waves.

### 3. Conclusion

This article demonstrates circular dichroism in a novel chiral metamaterial with twisted S-shaped rings rotated in quadrature on the top and bottom layers of FR4 substrate. RHCP and LHCP incident waves propagate with different transmission coefficients through the proposed metasurface. Due to non-reciprocity and lack of mirror plane symmetry, the asymmetric transmission of RHCP and LHCP waves takes place for incidence both on the front and back layers. Circular dichroism has widespread applications in the characterization of biological molecules.

### 4. References

1. Liqiao Jing, Zuoqia Wang, Yihao Yang, Bin Zheng, Yongmin Liu, and Hongsheng Chen, "Chiral metamirrors for broadband spin-selective absorption," *Applied Physics Letters* **110**, 23 2017, 231103.
2. Zhaofeng Li, Rongkuo Zhao, Thomas Koschny, Maria Kafesaki, Kamil Boratay Alici, Evrim Colak, Humeyra Caglayan, Ekmel Ozbay, and C. M. Soukoulis, "Chiral metamaterials with negative refractive index based on four "U" split ring resonators," *Applied Physics Letters* **97**, 8 2010, 081901.
3. Bingnan Wang, Jiangfeng Zhou, Thomas Koschny, Maria Kafesaki, and Costas M. Soukoulis, "Chiral metamaterials: simulations and experiments," *Journal of Optics A: Pure and Applied Optics* **11**, 11, 2009, 114003.
4. Yong Zhi Cheng, Yong Li Yang, Yu Jie Zhou, Zhe Zhang, Xue Song Mao, and Rong Zhou Gong, "Complementary Y-shaped chiral metamaterial with giant optical activity and circular dichroism simultaneously for terahertz waves," *Journal of Modern Optics* **63**, 17, 2016, 1675-1680.
5. Yongzhi Cheng, Fu Chen, and Hui Luo, "Multi-band giant circular dichroism based on conjugated bilayer twisted-semicircle nanostructure at optical frequency," *Physics Letters A* **384**, 19, 2020, 126398.
6. Yu Qu, Lishun Huang, Li Wang, and Zhongyue Zhang, "Giant circular dichroism induced by tunable resonance

in twisted Z-shaped nanostructure," *Optics Express* **25**, 5 2017, 5480-5487.

7. Yubin Ding, GuoPing Zhang, and Yongzhi Cheng, "Giant optical activity and negative refractive index in the terahertz region using complementary chiral metamaterials," *Physica Scripta* **85**, 6, 2012, 065405.